

The Higgs condensate as a quantum liquid: Comparison with the ATLAS full Run 2 data

Paolo Cea ¹

INFN - Sezione di Bari, Via Amendola 173 - 70126 Bari, Italy

Abstract

Recently, we proposed to picture the Higgs condensate of the Standard Model as a quantum liquid analogous to the superfluid Helium II. In this scenario the Higgs condensate excitations resemble closely two Standard Model Higgs bosons. The lightest Higgs boson was already identified with the LHC narrow resonance at 125 GeV. Concerning the heavy Higgs boson, we found preliminary evidence in our previous phenomenological analysis in the so-called golden channel. In the present note we compared our proposal to the full Run 2 data set released recently by the ATLAS Collaboration. Even though we do not found a clear statistical evidence for our Standard Model heavy Higgs, we found that our theoretical proposal is still in accordance with the available observations.

Keywords: Higgs Boson; Large Hadron Collider

PACS Nos.: 11.15.Ex; 14.80.Bn; 12.15.-y

¹Electronic address: paolo.cea@ba.infn.it

1 Introduction

In a recent article [1] we advanced the proposal that the Higgs condensate of the Standard Model should be considered like a relativistic quantum fluid analogous to superfluid helium. As discussed at length in Ref. [1], we found that there are two different kind of Higgs condensate excitations that are similar to phonon and rotons in helium II. Moreover, in the dilute gas approximation these two Higgs condensate excitations behave like the Standard Model Higgs boson [2, 3, 4, 5] and an heavy Higgs boson with mass around 730 GeV. Interestingly enough, it is noteworthy that an alternative scenario for the two-Higgs picture has been recently advanced in Refs. [6, 7].

Previous analyses of the preliminary LHC Run 2 data in the so-called golden channel $H \rightarrow \ell^+ \ell^- \ell'^+ \ell'^-$ where $\ell, \ell' = e$ or μ , seems to favour some evidence of a broad scalar resonance with mass around 700 GeV that looks consistent with a heavy Higgs boson [8, 9, 10]. The aim of the present note is to upgrade our previous analyses to the full LHC Run 2 data set from the ATLAS Collaboration, considering that the CMS Collaboration has not yet released the Run 2 data at least in the phase-space regions relevant to our purposes. In particular we shall contrast our theoretical proposal to the latest ATLAS data assuming that the additional heavy Higgs boson (denoted as H) is produced via gluon-gluon fusion (GGF) processes in Sect. 2, or vector-boson fusion (VBF) processes in Sect. 3. Finally, in Sect. 4 we summarise the main results of the paper.

2 The gluon-fusion production mechanism

In our previous papers [1, 9] we showed that for large Higgs masses the main production processes are by vector-boson fusion and gluon-gluon fusion processes. Moreover, almost all the decay modes of the heavy Higgs boson H are given by the decays into W^+W^- and Z^0Z^0 with:

$$Br(H \rightarrow W^+W^-) \simeq 2 Br(H \rightarrow Z^0Z^0). \quad (2.1)$$

It is well established that the decay channels $H \rightarrow ZZ \rightarrow 4\ell$ (the golden channel) have very low branching ratios, nevertheless the presence of leptons allows to efficiently reduce the huge background due mainly to diboson production. Indeed, the four-lepton channel, albeit rare, has the clearest and cleanest signature of all the possible Higgs boson decay modes due to the small background contamination. Usually, it is assumed that an additional Higgs boson would be produced predominantly via gluon-gluon fusion (GGF) and vector-boson fusion (VBF) processes. Therefore, the events are classified into GGF and VBF categories and results are interpreted separately for the GGF and VBF production modes. A search for a new high-mass resonances decaying into electron or muon pairs has been performed the ATLAS experiment using data collected at $\sqrt{s} = 13$ TeV corresponding to an integrated luminosity of 36 fb^{-1} [14] and upgraded to 139 fb^{-1} [12].

In Fig. 1 we show the invariant mass distribution for the golden channel for the GGF category corresponding to 36 fb^{-1} (left panel) and 139 fb^{-1} (right panel). In order to be sensitive to the VBF production mode, for the 36.1 fb^{-1} data set, the ATLAS Collaboration [14] classified the events into four categories, namely one for the VBF production mode and three for the GGF production mode. If an event has two or more jets with p_T greater than 30 GeV, with the two leading jets j_1, j_2 well separated in the pseudo-rapidity η , i.e. $|\eta_{j_1 j_2}| > 3.3$, and having an invariant mass $m_{j_1 j_2} > 400$ GeV, then this event is

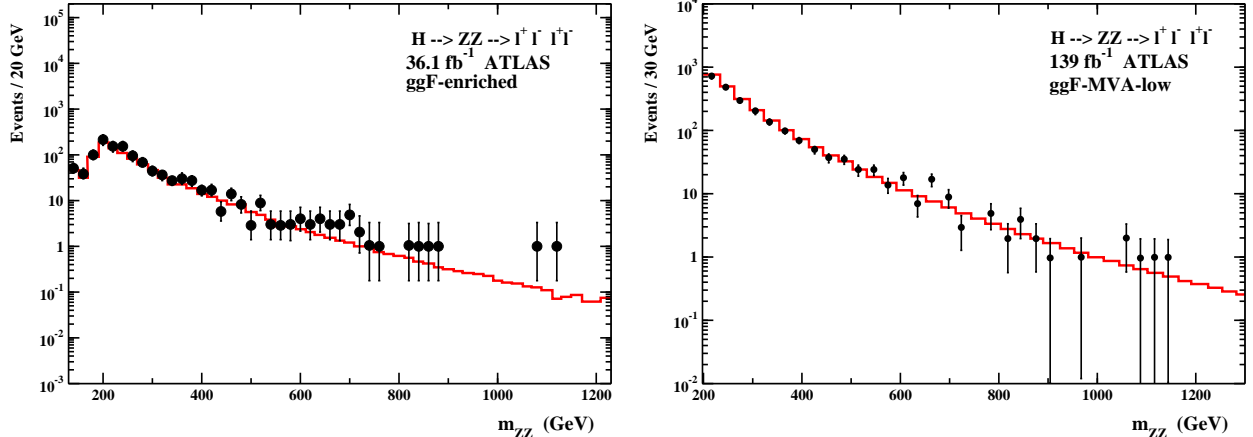


Figure 1: Distribution of the invariant mass m_{ZZ} for the GGF processes $H \rightarrow ZZ \rightarrow \ell\ell\ell\ell$ ($\ell = e, \mu$) corresponding to an integrated luminosity of $\mathcal{L} = 36.1 fb^{-1}$ (left panel) and $139 fb^{-1}$ (right panel). The data have been obtained from Fig. 4 (a) in Ref. [14] and Fig. 2 (d) in Ref. [12], respectively. The (red) continuous lines are the ZZ irreducible backgrounds.

classified into the VBF-enriched category. Otherwise the event is classified into one of the GGF-enriched categories. Such classification is used only in the search for a heavy scalar produced with the narrow width approximation.

On the other hand, for the full Run 2 data set the event classification targeting different production processes has been optimised using machine learning algorithms [12]. More precisely, to improve the sensitivity in the search of a heavy Higgs signal produced either in the VBF or in the GGF production mode, were used two classifiers, a VBF classifier and a GGF classifier. These classifiers were built with deep neural networks. The networks were trained by means of simulated signal events from a heavy Higgs boson with masses ranging from 200 GeV up to 1400 GeV in the narrow width approximation, and from the Standard Model continuous ZZ background.

From the event distributions we may easily obtain the signal distributions by subtracting the continuous irreducible ZZ backgrounds that constitute the main source of the Standard Model background in the invariant high-mass region. The results are displayed in Fig. 2. After that, we compare the observed signal distributions to our theoretical proposal. For the 2016 ATLAS data set, we see that the expected signal histogram is perfectly compatible with the data, but it is evident from Fig. 2, left panel, that the integrated luminosity is too low to claim an evidence of our heavy Higgs boson. As concern the full data set, in Fig. 2, right panel, we compare the expected signal distribution to the data. For the comparison we have taken into account that the selection cuts applied by the ATLAS Collaboration to the full Run 2 data set are more stringent with respect to the preliminary data. This can be seen by looking at the number of events in the the high-mass region $m_{ZZ} > 600$ GeV. From the $36.1 fb^{-1}$ data we infer that there are about 28 events. Since the luminosity increases by a factor $139/36.1 \simeq 3.85$, we should have about 108 events. Actually, we found that the full Run 2 data set has about 75 events in the high-mass region. To take care of this we introduce an effective efficiency factor:

$$\eta_{eff}^{GGF} \simeq \frac{75}{108} \simeq 0.70 \quad , \quad (2.2)$$

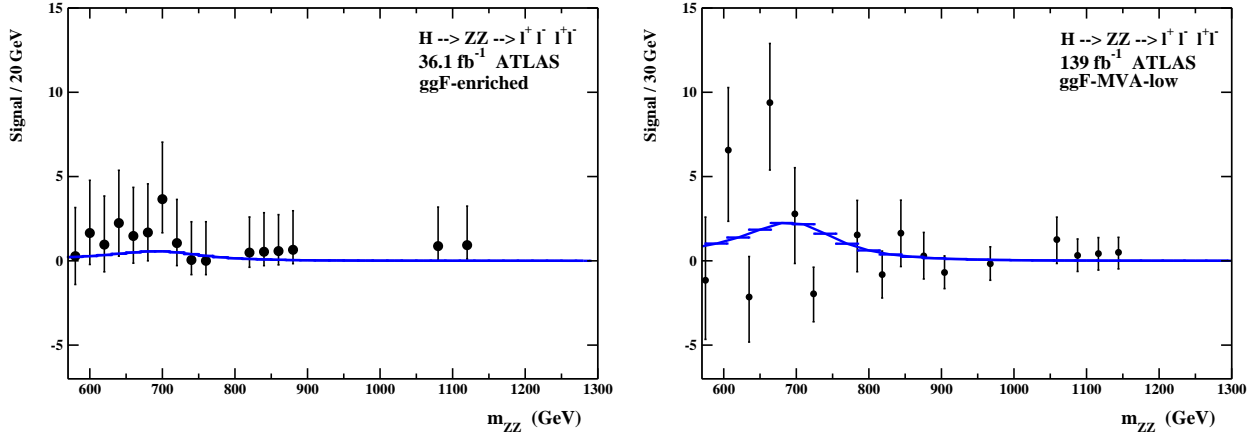


Figure 2: Comparison to the Run 2 data of the distribution of the invariant-mass m_{ZZ} distribution in the high-mass region $m_{ZZ} \gtrsim 600 \text{ GeV}$ for the GGF processes $H \rightarrow ZZ \rightarrow \ell\ell\ell\ell$ ($\ell = e, \mu$) with integrated luminosity 36.1 fb^{-1} (left panel) and 139 fb^{-1} (right panel). The signal distribution has been obtained from the relevant ATLAS event distributions by subtracting the ZZ backgrounds.

and scaled the production cross section accordingly. After that we compare the theoretical distribution to the data. Looking at Fig. 2, right panel, we see that the data do display some broad structure around $m_{ZZ} \simeq 700 \text{ GeV}$ that compares reasonably with the theoretical expectations. To be quantitative, we may estimate the total number of events in the invariant mass interval $m_{ZZ} > 700 \text{ GeV}$ and compare with our theoretical expectations. We find:

$$N_{sign}^{exp}(m_{ZZ} > 600 \text{ GeV}) \simeq 19.68_{-8.52}^{+7.44}, \quad N_{sign}^{th} = 12.20 \quad GGF \quad \mathcal{L} = 139 \text{ fb}^{-1} \quad (2.3)$$

where the quoted errors have been obtained by adding in quadrature the experimental errors.² Even though the observed and predicted event counts are in quite good agreement, the background-only hypothesis is still consistent with observations, albeit at about two standard deviations.

According to Eq. (2.1), the main decay mode of a heavy Higgs boson is the decays into two W vector bosons. Thus, the most stringent constraints should arise from the experimental searches for a heavy Higgs boson decaying into two W gauge bosons. In fact, in our previous paper [1] we compared our theoretical expectations to the search for neutral heavy resonances in the $WW \rightarrow e\nu\mu\nu$ decay channel performed by the ATLAS Collaboration using proton-proton collision data at $\sqrt{s} = 13 \text{ TeV}$ and corresponding to an integrated luminosity of 36.1 fb^{-1} [14]. To upgrade to the full Run 2 data set, we may use the recent results presented by the ATLAS Collaboration on the search of heavy resonances decaying into two vector bosons WW, ZZ or WZ using collected data corresponding to an integrated luminosity of 139 fb^{-1} [15]. We will focus on the results for the search of heavy neutral scalar resonance, called the Radion, which appears in some theoretical models and which, indeed, can decay into WW or ZZ with a branching ratio approximatively given by Eq. (2.1). Moreover, the Radion-like scalar resonances couple to the Standard Model

²Strictly speaking, the combination of measurements with asymmetric errors should be implemented by combining the likelihood functions (for instance, see Ref. [13]). Here, we are adopting a conservative attitude for adding errors in quadrature leads, in general, to an overestimate of the statistical errors.

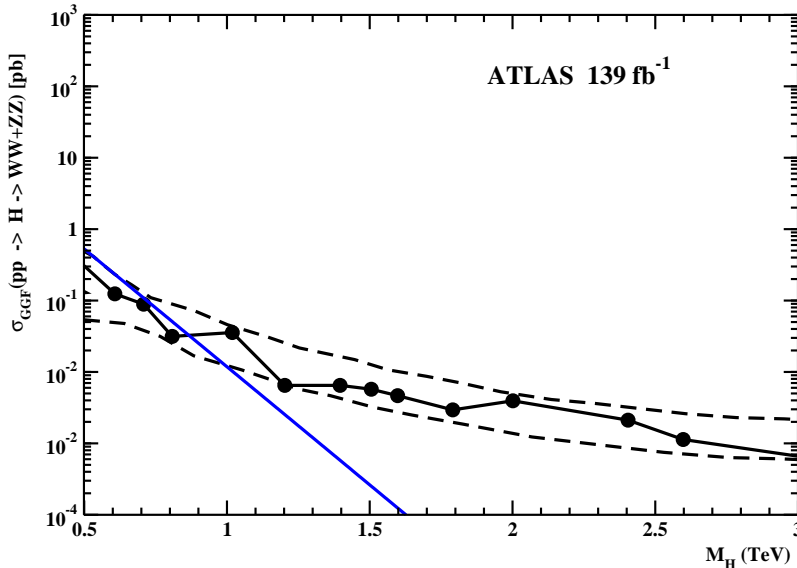


Figure 3: Limits on the GGF production cross section times the branching fraction for the processes $pp \rightarrow H \rightarrow VV$, $V = W, Z$. The data have been taken from Fig. 12 (a) in Ref. [15]. The dashed lines demarcate the 95 % confidence level region of the expected Standard Model background. Full circles represent the observed signal. The continuous (blu) line is our theoretical estimate for the gluon-gluon fusion production cross section times the branching ratio $\text{Br}(H \rightarrow WW + ZZ)$.

fermions and gauge bosons with strengths similarly to a heavy Higgs boson. Considering that these heavy scalar resonances have a rather narrow widths, we can consider the observed limits on the production processes as indicative of the production of a heavy Standard Model heavy Higgs boson in the narrow width approximation.

In Fig. 3 we display the observed limits at 95 % confidence level on the heavy Higgs boson production cross section times the branching fraction $Br(H \rightarrow WW + ZZ)$ for the gluon-gluon fusion production mechanisms in the narrow width approximation as reported in Ref. [15]. For comparison, in Fig. 3 we also report our estimate for the product of the gluon-gluon fusion production cross section times the branching ratio for the decay of the heavy Higgs boson into two vector bosons, after taking into account the reduced efficiency as estimated in Eq. (2.2). Looking at Fig. 3, it is evident that, in the relevant mass range, our theoretical cross section is compatible with the observed limits. On the other hand, the observed gluon-gluon fusion cross section falls within the $\pm 2\sigma$ ranges around the expected limit for the Standard Model background-only hypothesis.

3 The vector boson production mechanism

In the present Section we focus on the vector-boson fusion production mechanism. In Fig. 4 we display the invariant mass distribution for the golden channel for the VBF category corresponding to 36 fb^{-1} (left panel) and 139 fb^{-1} (right panel). It is, now, worthwhile to comment on the effects of the tightly selection cuts applied by the ATLAS Collaboration on the full Run 2 data. In fact, notwithstanding the integrated luminosity has increased by a factor of about four, the number of events in the the high-mass region

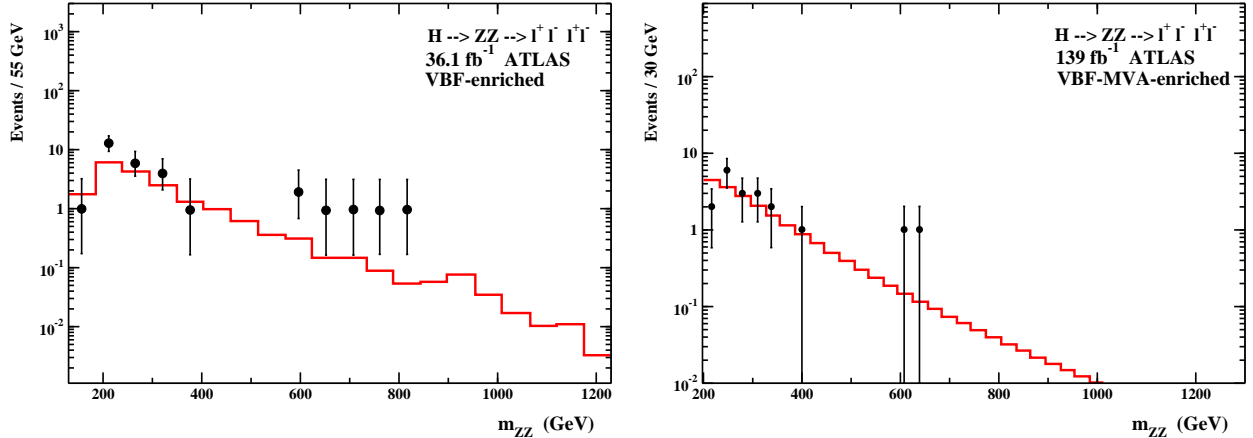


Figure 4: Distribution of the invariant mass m_{ZZ} for the VBF processes $H \rightarrow ZZ \rightarrow \ell\ell\ell\ell$ ($\ell = e, \mu$) corresponding to an integrated luminosity of $\mathcal{L} = 36.1 fb^{-1}$ (left panel) and $139 fb^{-1}$ (right panel). The data have been obtained from Fig. 4 (b) in Ref. [14] and Fig. 2 (e) in Ref. [12], respectively. The (red) continuous lines are the ZZ irreducible backgrounds.

$m_{ZZ} > 600$ GeV decreases from four to two. This corresponds to an effective efficiency factor:

$$\eta_{eff}^{VBF} \simeq 0.13 \quad . \quad (3.1)$$

In our opinion, these drastic effects derive from the event selection strategy that, for the full Run 2 data set, is built with deep neural networks. It turns out that the neural networks are trained using the discriminating variables on simulated events from the decays of a heavy Higgs bosons with masses $200 \text{ GeV} \leq m_H \leq 1400 \text{ GeV}$ within the narrow width approximation, and the Standard Model ZZ background. We suspect that the event selection in the high invariant-mass region is strongly biased due to the narrow width approximation and the strongly suppressed background of the Standard Model used in the training procedure of the neural networks. Indeed, the invariant-mass distribution from decays of our Higgs boson is a rather broad structure around 700 GeV that resemble more closely an almost continuous distribution than the distribution arising from the decays of a narrow-width Higgs boson. Now, Fig. 4, right panel, shows that the Standard Model ZZ background is strongly suppressed in the high invariant-mass region for Higgs production via the vector-boson fusion process. Therefore, it is conceivable that eventual signals from our Higgs boson could have been rejected by the event selection cuts.

As in the previous Section, from the event distributions we extract the signal distributions by subtracting the ZZ background (see Fig. 5) and compare with the expected distribution. For the 2016 ATLAS data set, we see that the expected signal histogram is perfectly compatible with the data even though the integrated luminosity is too low to support the heavy Higgs boson with a significative statistical significance. As concern the full data set, in Fig. 5, right panel, we compare the expected signal distribution, scaled by the effective efficiency factor Eq. (3.1), to observations. Again, we see that there is not enough significancy to claim an evidence. This is confirmed more concretely by comparing the expected and observed number of events in the high invariant-mass region:

$$N_{sign}^{exp}(m_{ZZ} > 600 \text{ GeV}) \simeq 1.76_{-1.42}^{+1.36}, \quad N_{sign}^{th} = 3.48 \quad VBF \quad \mathcal{L} = 139 fb^{-1} \quad . \quad (3.2)$$

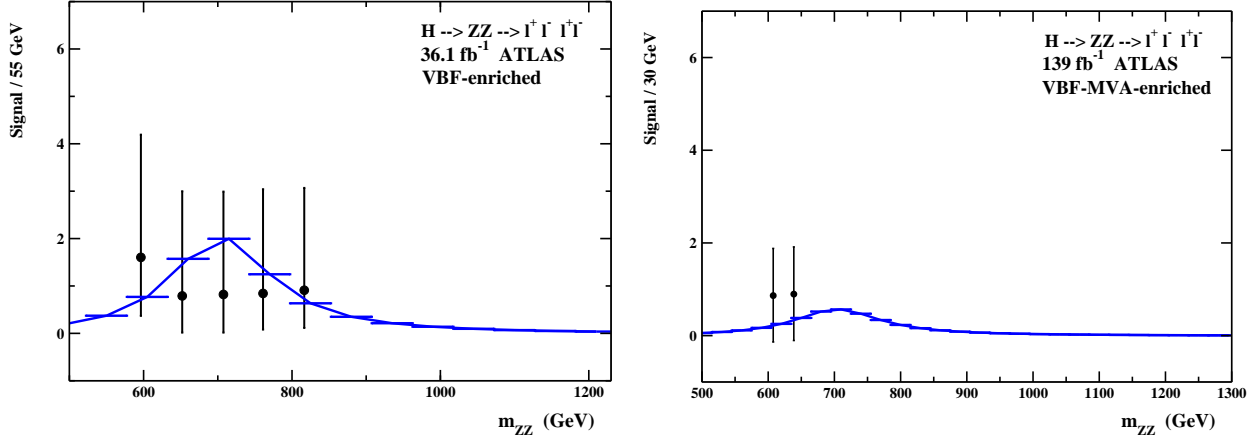


Figure 5: Comparison to the Run 2 data of the invariant-mass m_{ZZ} distribution in the high-mass region $m_{ZZ} \gtrsim 600 \text{ GeV}$ for the VBF processes $H \rightarrow ZZ \rightarrow \ell\ell\ell\ell$ ($\ell = e, \mu$) with integrated luminosity 36.1 fb^{-1} (left panel) and 139 fb^{-1} (right panel). The signal distribution has been obtained from the relevant ATLAS event distributions by subtracting the ZZ backgrounds.

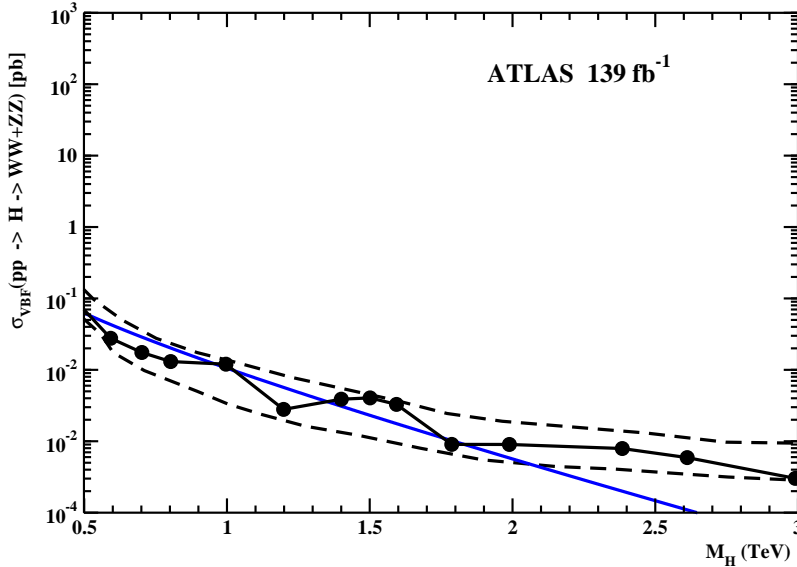


Figure 6: Limits on the VBF production cross section times the branching fraction for the processes $pp \rightarrow H \rightarrow VV$, $V = W, Z$. The data have been taken from Fig. 12 (b) in Ref. [15]. The dashed lines demarcate the 95 % confidence level region of the expected Standard Model background. Full circles represent the observed signal. The continuous (blu) line is our theoretical estimate for the gluon-gluon fusion production cross section times the branching ratio $\text{Br}(H \rightarrow WW + ZZ)$.

Finally, In Fig. 6 we display the observed limits at 95 % confidence level on the heavy Higgs boson production cross section times the branching fraction $Br(H \rightarrow WW + ZZ)$ for the vector-boson fusion production mechanism in the narrow width approximation as reported in Ref. [15]. For comparison, we also report our estimate for the product of the VBF production cross section times the branching ratio for the decay of the heavy Higgs boson into two vector bosons, after taking into account the reduced efficiency as estimated in Eq. (3.1). Looking at Fig. 6, it is evident that, in the relevant mass range, both our theoretical cross section and the Standard Model background-only hypothesis are compatible with the observed limits.

4 Summary and conclusions

In our previous paper we proposed to picture the Higgs condensate of the Standard Model as a quantum liquid analogous to the superfluid helium. In this scenario the Higgs condensate excitations behave as two Higgs bosons. The light Higgs boson was already identified with the LHC narrow resonance at 125 GeV. As concern the heavy Higgs boson, we found preliminary evidence in our previous phenomenological analysis in the golden channel of the preliminary LHC Run 2 data from ATLAS and CMS Collaborations. In the present note we compared our proposal to the full Run 2 data set released recently by the ATLAS Collaboration. We do not found a clear statistical evidence for our Standard Model heavy Higgs. At best we found a hint of a signal in the gluon-gluon fusion Higgs production mechanism. We argued that there is not enough sensitivity to detect the signal in vector-boson fusion mechanism mainly due to tight event-selection cuts. In any case, we concluded that our theoretical proposal is still in accordance with the available observations.

References

- [1] P. Cea, The Higgs Condensate as a Quantum Liquid, International Journal of Theoretical Physics **59**, 3310 (2020)
- [2] F. Englert and R. Brout, Broken Symmetry and the Mass of Gauge Vector Mesons, Phys. Rev. Lett. **13**, 321 (1964)
- [3] P. Higgs, Broken symmetries, massless particles and gauge fields, Phys. Lett. **12**, 132 (1964)
- [4] G. Guralnik, C. Hagen and T. Kibble, Global Conservation Laws and Massless Particles, Phys. Rev. Lett. **13**, 585 (1964)
- [5] P. Higgs, Spontaneous Symmetry Breakdown without Massless Bosons, Phys. Rev. **145**, 1156 (1966)
- [6] Maurizio Consoli and Leonardo Cosmai, The mass scales of the Higgs field, Int. J. Mod. Phys. A **35** 2050103 (2020)
- [7] Maurizio Consoli and Leonardo Cosmai, Spontaneous Symmetry Breaking and Its Pattern of Scales, Symmetry **12**, 2037 (2020)

- [8] P. Cea, The H_T Higgs boson at the LHC Run 2, arXiv:1707.05605 [hep-ph] (2017)
- [9] P. Cea, Evidence of the true Higgs boson H_T at the LHC Run 2, Mod. Phys. Lett. A **34**, 1950137 (2019)
- [10] F. Richard, Indications for extra scalars at LHC? – BSM physics at future e^+e^- colliders, arXiv:2001.04770 [hep-ex] (2020)
- [11] M. Aaboud *et al.*, the ATLAS Collaboration, Search for heavy ZZ resonances in the $\ell^+\ell^-\ell^+\ell^-$ and $\ell^+\ell^-\nu\bar{\nu}$ final states using proton-proton collisions at $\sqrt{s} = 13$ TeV with the ATLAS detector, Eur. Phys. J. C **78**, 293 (2018)
- [12] G. Aad *et al.*, the ATLAS Collaboration, Search for heavy resonances decaying into a pair of Z bosons in the $\ell^+\ell^-\ell^+\ell^-$ and $\ell^+\ell^-\nu\bar{\nu}$ final states using 139 fb $^{-1}$ of proton-proton collisions at $\sqrt{s} = 13$ TeV with the ATLAS detector, Eur. Phys. J. C **81**, 332 (2021)
- [13] Roger John Barlow, Statistics for Particle Physics CERN Yellow Rep. School Proc. **5**, 149 (2020), Contribution to: AEPSHEP 2018, arXiv: 1905.12362 [physics.data-an]
- [14] M. Aaboud, *et al.*, the ATLAS Collaboration, Search for heavy resonances decaying into WW in the $e\nu\mu\nu$ final state in pp collisions at $\sqrt{s} = 13$ TeV with the ATLAS detector, Eur. Phys. J. C **78**, 24 (2018)
- [15] G. Aad *et al.*, the ATLAS Collaboration, Search for heavy diboson resonances in semileptonic final states in pp collisions at $\sqrt{s} = 13$ TeV with the ATLAS detector, Eur. Phys. J. C **80**, 1165 (2020)